Capacity Analysis and Rate Maximization Design in RIS-Aided Uplink Multi-User MIMO

Capacity Analysis and Rate Maximization Design in RIS-Aided Uplink Multi-User MIMO

Wei Jiang*† and Hans D. Schotten†*

*Intelligent Networking Research Group, German Research Center for Artificial Intelligence (DFKI), Germany

†Department of Electrical and Computer Engineering, Technische Universität (TU) Kaiserslautern, Germany

Abstract

Reconfigurable intelligent surface (RIS) has recently drawn intensive attention due to its potential of simultaneously realizing high spectral and energy efficiency in a sustainable way. This paper focuses on the design of efficient transmission methods to maximize the uplink sum throughput in a RIS-aided multi-user multi-input multi-output (MU-MIMO) system. To provide an insightful basis, the channel capacity of RIS-aided MU-MIMO is theoretically analyzed. Then, the conventional transmission schemes based on orthogonal multiple access are presented as the baseline. From the information-theoretic perspective, we propose two novel schemes, i.e., *joint transmission* based on the semidefinite relaxation of quadratic optimization problems and *opportunistic transmission* relying on the best user selection. The superiority of the proposed schemes over the conventional ones in terms of achievable rates is justified through simulation results.

I. Introduction

Motivated by the big commercial success of the fourth generation a.k.a 3GPP LTE-Adavnced [1]–[3] and the fifth generation (5G) technology [4]–[14], both the academia and industry have already shifted their focus towards the sixth generation (6G) [15]–[18] and enthusiastically initiated many pioneering research programs although 5G is still on its way to being deployed across the world. To support disruptive use cases beyond 2030, such as holographic communications, extended reality, artificial intelligence [19]–[28], Tactile Internet, Internet of Things [29]–[35], multi-sense experience, metaverse, digital twin, and block-chain [36], 6G needs to meet more stringent performance requirements than its predecessor, e.g., a peak data rate of 1 terabits-per-second (Tbps), a massive connection density of 10^7 devices per km^2, and high-accuracy positioning, sensing [37]–[39], identification and tracking [40]–[42]. Traditionally, three major approaches, i.e., *(1) Deploying Dense and Heterogeneous Networks*, *(2) Installing Massive Antennas for Extreme Spectral Efficiency*, and *(3) Enlarging Bandwidth* can effectively improve coverage and capacity. Nevertheless, these approaches incur high capital and operational expenditures, unaffordable energy consumption, and severe network interference. Given these limitations, further evolving along the old track is hard to fully achieve stringent 6G requirements. Therefore, it is highly desirable to develop a revolutionary technology to realize sustainable capacity and performance growth with affordable cost, low complexity, and efficient energy consumption.

Along with other 6G-potential technologies, such as terahertz communications [43]–[45] and cell-free massive MIMO [46]–[51], a disruptive technique referred to as reconfigurable intelligent surface (RIS) has recently attracted intensive attention from academia and industry due to its potential to simultaneously meet the aforementioned demands [52]–[55]. Through smartly adjusting the reflection coefficients of a large number of reconfigurable elements over a planar meta-surface [56], an on-demand propagation environment is achieved for signal amplification or interference suppression, so as to improve the performance of

wireless communications. Since the reflecting elements are nearly passive, low-cost, and lightweight, the RIS is a green and cost-efficient technology. It enables sustainable capacity and performance growth for legacy 5G networks and the forthcoming 6G system [16], [18].

Prior works on RIS-aided communications mostly focus on point-to-point communications that consider a base station (BS), a surface, and a single user. Depending on the number of antennas, the research works span from single-input single-output (SISO) to multi-input multi-output (MIMO). Nevertheless, a practical wireless system needs to accommodate many users simultaneously, imposing the necessity of studying multi-user MIMO (MU-MIMO). There has been a few recent works on this topic. The authors of [57] developed a novel technique for passive beamforming and information transfer in RIS-aided MU-MIMO systems. In [58], a trade-off between energy and spectral efficiency in MU-MIMO uplink communications aided by a discrete-phase-shift RIS is discussed. The design of linear or nonlinear receivers for MU-MIMO systems aided by multiple RISs is studied in [59]. Zheng *et al.* aimed to unveil the full potential of multi-RIS assisted wireless networks by studying a double-RIS multi-user communication system with cooperative passive beamforming in [60]. The work [61] jointly optimizes the uplink transmit beamforming and the phase-shift matrix to maximize the system energy efficiency under partial channel state information (CSI). In [62], the effect of double RISs in improving the spectral efficiency of an MU-MIMO network operating in millimeter wave is investigated. Joint beamforming and modulation design for embedding extra data into carrier signals from the BS to the RIS in a downlink MU-MIMO network is proposed in [63]. The work [64] presents a novel symbiotic radio system on the basis of RIS-aided MU-MIMO to enhance the primary transmission and simultaneously transmit its own information by back-scattering modulation. In addition, some other works such as [65], [66] focus on one of the fundamental challenges, namely the acquisition of cascaded channel information, in RIS-assisted MU-MIMO systems.

This paper focuses on designing efficient transmission for a RIS-aided MU-MIMO system with the aim of maximizing its uplink sum throughput. To provide an insightful basis, an information-theoretic analysis in terms of the sum capacity is theoretically conducted. The conventional orthogonal multiple access (OMA) schemes, including time-division multiple access (TDMA) and frequency-division multiple access (FDMA), are presented as the baseline. Then, we propose two novel schemes, i.e., *joint transmission (JT)* based on the semidefinite relaxation of quadratic optimization problems and *opportunistic transmission (OT)* relying on the best user selection. The superiority of the proposed schemes over OMA in terms of achievable sum rate is justified through Monte-Carlo simulation.

The rest of the paper is organized as follows: Section II introduces the system model. Section III analyzes the channel capacity. In Section IV, the proposed JT and OT schemes are elaborated in comparison with the OMA schemes. Simulation setup and numerical results are demonstrated in Section V. Finally, Section VI concludes this paper.

II. System Model

Consider a RIS-aided multi-user MIMO communications system, which comprises an N_b-antenna BS, K single-antenna user equipment (UE), and a surface with N_s reconfigurable elements [67]. MU-MIMO is an *asymmetric* system, where the downlink from a BS to several UEs is referred to as *Gaussian MIMO broadcast channel*, while the uplink from multiple UEs to the BS is called *Gaussian MIMO multiple access channel*. This paper merely focuses on the uplink transmission while its analysis and development also provide some meaningful insights on the downlink transmission.

As demonstrated in Fig.1, multiple UEs simultaneously send its respective signal towards the BS over the same time-frequency resource. For the sake of analysis, we do not consider linear beamforming [68]–[74] over the antenna array and assume the BS

is equipped with a single antenna. The BS acquires the uplink instantaneous CSI through estimating the pilot signals during the uplink training period. To facilitate the theoretical analysis, the BS is assumed to perfectly know the CSI of all involved channels, as prior works [57]- [64]. Moreover, we do not consider the impact of channel aging or outdated channel information in fast-fading environments [75]–[83], and assume narrowband communications, where the channels follow frequency-flat block fading. A wideband channel suffering from frequency selectivity can be transformed into a set of narrowband channels through orthogonal frequency-division multiplexing (OFDM) [84]–[90], making the assumption of flat fading reasonable.

The RIS is equipped with a smart controller that adaptively adjusts the phase shift of each reflecting element according to the knowledge of CSI. Mathematically, a typical element $n \in \{1, 2, \ldots, N_s\}$ is modeled by a reflection coefficient $\epsilon_n = a_n e^{j\theta_n}$, where $\theta_n \in [0, 2\pi)$ denotes an induced phase shift, and $a_n \in [0, 1]$ stands for amplitude attenuation. Although the practical RIS implementation supports a finite number of discrete phase shifts, only a few phase-control bits (e.g., 2 bits as illustrated in [53]) are sufficient for achieving near-optimal performance as continuous phase shifts. Without loss of generality, we use continuous phase shifts hereinafter for simplicity. As mentioned by [67], $a_n = 1$, $\forall n$ is the optimal setting that maximizes the signal strength and simplifies the implementation. Therefore, the RIS optimization focuses on a diagonal phase-shift matrix defined as $\mathbf{\Phi} = \text{diag}\{e^{j\theta_1}, \ldots, e^{j\theta_{N_s}}\}$.

We use $s_k \in \mathbb{C}$ to denote the information symbol from user k, satisfying $\mathbb{E}[|s_k|^2] \leqslant P_k$, where P_k denotes the power constraint of user k. All information symbols form a transmitted vector $\mathbf{s} \in \mathbb{C}^{K\times 1} = [s_1, s_2, \ldots, s_K]^T$. Let $\mathbf{D} \in \mathbb{C}^{N_b\times K}$ denote the channel matrix from K users to N_b receive antennae at the BS, and $\mathbf{d}_k \in \mathbb{C}^{N_b\times 1}$ denotes the spatial signature of user k impinged on the BS antenna array, we have $\mathbf{D} = [\mathbf{d}_1, \mathbf{d}_2, \ldots, \mathbf{d}_K]$. Let $\mathbf{G} \in \mathbb{C}^{N_s\times K}$ denote the channel matrix from K users to N_s reflecting elements, we have $\mathbf{G} = [\mathbf{g}_1, \mathbf{g}_2, \ldots, \mathbf{g}_K]$, where $\mathbf{g}_k \in \mathbb{C}^{N_s\times 1}$ represents the spatial signature of user k impinged over the RIS. Similarly, we write $\mathbf{F} \in \mathbb{C}^{N_b\times N_s}$ to denote the channel matrix from the RIS to the BS. Without losing generality, any entry within these channel vectors or matrices is modeled as a circularly symmetric complex Gaussian random variable denoted by $X \sim \mathcal{CN}(\mu, \sigma_c^2)$, where μ denotes the mean, and σ_c^2 is the average channel (power) gain.

The overall system can be modelled as

$$\mathbf{y} = \Big(\mathbf{F}\mathbf{\Phi}\mathbf{G} + \mathbf{D}\Big)\mathbf{s} + \mathbf{n}, \tag{1}$$

where $\mathbf{y} = [y_1, y_2, \ldots, y_{N_b}]^T$ stands for the received vector, and $\mathbf{n} \in \mathcal{CN}(\mathbf{0}, \sigma_n^2\mathbf{I}_{N_b})$ is independent and identically distributed (*i.i.d.*) additive white Gaussian noise (AWGN) with zero mean and variance σ_n^2. Decomposing (1), the signal model can be rewritten as an alternative form

$$\mathbf{y} = \sum_{k=1}^{K}\Big(\mathbf{F}\mathbf{\Phi}\mathbf{g}_k + \mathbf{d}_k\Big)s_k + \mathbf{n}. \tag{2}$$

III. Capacity Analysis

In a point-to-point system, the channel capacity provides a measure of the performance limit: reliable communications with an arbitrarily small error probability can be achieved at any rate $R < C$, whereas reliable communications are impossible when $R > C$. For a multi-user system consisting of a BS and K UEs, the concept is extended to a similar performance metric called *a capacity region* [91]. It is characterized by a K-dimensional space $\mathfrak{C} \in \mathbb{R}_+^K$, where $\mathbb{R}_+$ denotes the set of non-negative real-valued numbers, and $\mathfrak{C}$ is the set of all K-tuples $(R_1, R_2, \ldots, R_K)$ such that a generic user k can reliably communicate at rate R_k

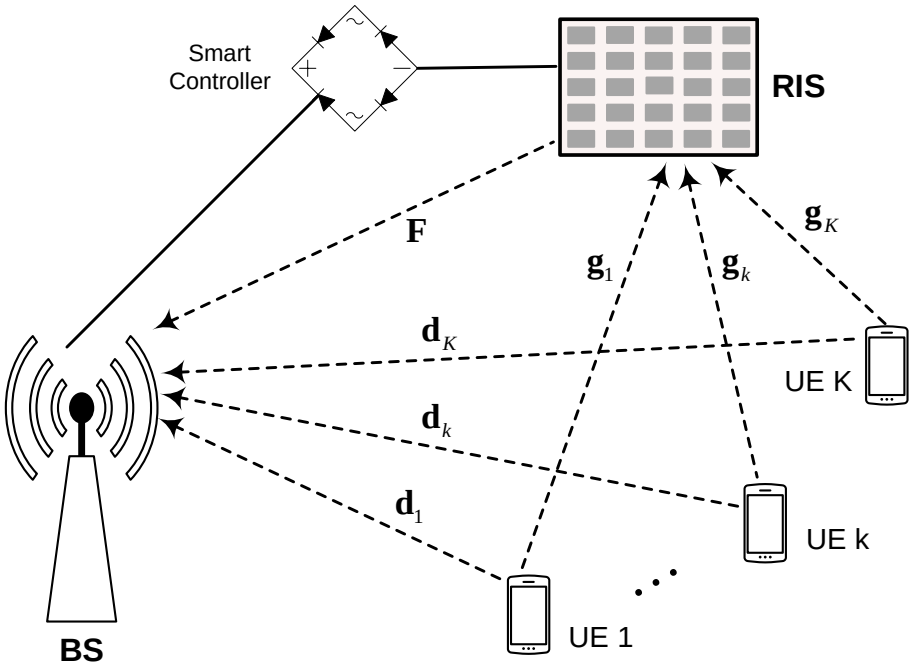

Fig. 1. Schematic diagram of the uplink transmission of a RIS-aided MU-MIMO system consisting of a BS, a RIS, and K users.

simultaneously with others. Due to the shared transmission resource, there is a trade-off: if one desires a higher rate, some of other users have to lower their rates. From this capacity region, a performance metric can be derived, i.e., the sum capacity

$$C_{sum} = \max_{(R_1,R_2,\ldots,R_K)\in\mathfrak{C}} \left(\sum_{k=1}^{K} R_k \right), \tag{3}$$

indicating the maximum total throughput that can be achieved.

The achievable rate of a typical user is limited by the *single-user bound*, which is the capacity of the point-to-point link with the other users absent from the system. From (2), we have

$$R_k < \log \left[1 + \frac{\|\mathbf{F}\mathbf{\Phi}\mathbf{g}_k + \mathbf{d}_k\|^2 P_k}{\sigma_n^2} \right], \ \forall\, k. \tag{4}$$

In addition, any combination of user rates are constrained by

$$\sum_{k\in\mathcal{S}} R_k < \log\det \left[\mathbf{I}_{N_b} + \frac{\sum_{k\in\mathcal{S}} \|\mathbf{F}\mathbf{\Phi}\mathbf{g}_k + \mathbf{d}_k\|^2 P_k}{\sigma_n^2} \right],$$
$$\forall \mathcal{S} \in \left\{1, 2, \ldots, K\right\}. \tag{5}$$

For the ease of notation, we write $\mathbf{h}_k = \left(\mathbf{F}\mathbf{\Phi}\mathbf{g}_k + \mathbf{d}_k\right)$ to denote the effective channel from user k to the BS with the aid of the RIS. The capacity region is now a K-dimensional polyhedron, which can be mathematically described by

$$\mathfrak{C} = \left\{ (R_1, \ldots, R_K) \in \mathbb{R}_+^K \left| \begin{array}{c} \sum_{k\in\mathcal{S}} R_k < \log\det \left[\mathbf{I}_{N_b} + \frac{\sum_{k\in\mathcal{S}} \|\mathbf{h}_k\|^2 P_k}{\sigma_n^2} \right] \\ \forall \mathcal{S} \in \left\{1, 2, \ldots, K\right\} \end{array} \right. \right\}. \tag{6}$$

The *sum capacity* of a RIS-aided MU-MIMO system can be given by

$$C_{sum} = \log\det\left[\mathbf{I}_{N_b} + \frac{\sum_{k=1}^{K} \|\mathbf{F}\mathbf{\Phi}\mathbf{g}_k + \mathbf{d}_k\|^2 P_k}{\sigma_n^2}\right]. \tag{7}$$

It is not difficult to derive that the instantaneous channel gain of multiple users is equivalent to an overall channel gain, namely

$$\sum_{k=1}^{K} \|\mathbf{F}\mathbf{\Phi}\mathbf{g}_k + \mathbf{d}_k\|^2 = \|\mathbf{F}\mathbf{\Phi}\mathbf{G} + \mathbf{D}\|^2 . \tag{8}$$

If all users have the same power constraint, i.e., $P_k = P_u$, $\forall k$, the sum capacity in (7) is rewritten as

$$C_{sum} = \log\det\left[\mathbf{I}_{N_b} + \frac{\|\mathbf{F}\mathbf{\Phi}\mathbf{G} + \mathbf{D}\|^2 P_u}{\sigma_n^2}\right]. \tag{9}$$

IV. Sum-Rate Maximization Design

The aim of this paper is to design efficient transmission for the maximization of the sum rate in the uplink RIS-aided MU-MIMO systems. From (9), the sum capacity is a function of $\mathbf{\Phi}$, resulting in the following optimization formula

$$\begin{aligned} \max_{\mathbf{\Phi}} \quad & \|\mathbf{F}\mathbf{\Phi}\mathbf{G} + \mathbf{D}\|^2 \\ \text{s.t.} \quad & \theta_n \in [0, 2\pi),\ \forall n = 1, \ldots, N_s, \end{aligned} \tag{10}$$

which is mathematically intractable.

Fortunately, it is observed that the BS-RIS link generally has a strong line-of-sight (LOS) path since both nodes are stationary, and their deployment locations are deliberately selected without any blockage in-between. In contrast to randomly distributed, moving UEs, the BS-RIS channel exhibits high correlation and sparsity. Furthermore, if the BS applies a correlated antenna array, e.g., with a small inter-element spacing of half wavelength, the channel can be modelled as the product of the channel vector of the reference antenna and the steering vector of the array [68]. Therefore, the BS-RIS link can be represented by the channel vector $\mathbf{f} \in \mathbb{C}^{1\times N_s}$ between the reference antenna and the RIS. Accordingly, the direct channel is degraded from $\mathbf{D}$ to $\mathbf{d} \in \mathbb{C}^{1\times K}$. As a result, (10) is simplified to

$$\begin{aligned} \max_{\mathbf{\Phi}} \quad & \|\mathbf{f}\mathbf{\Phi}\mathbf{G} + \mathbf{d}\|^2 \\ \text{s.t.} \quad & \theta_n \in [0, 2\pi),\ \forall n = 1, \ldots, N_s. \end{aligned} \tag{11}$$

The objective function in (11) becomes solvable since it is quadratically constrained quadratic program (QCQP) optimization [92], based on which *joint transmission* is proposed. In addition, *opportunistic transmission* relying on the best user selection is also provided. For comparison, this section first presents the behaviours of the conventional OMA schemes including TDMA and FDMA in RIS-aided MU-MIMO systems.

A. Orthogonal Multiple Access

1) TDMA-RIS: It is a simple scheme by dividing the signaling dimension along the time axis into K orthogonal slots. Using the round-robin scheduling, each user cyclically accesses to its assigned slot. A general user k transmits s_k at the k^{th} slot while other users keep silent. According to [93], a RIS element made by positive-intrinsic-negative (PIN) diodes has a maximal switching frequency of 5 MHz, much faster than the shifting of time slots typically on the order of millisecond (ms). It implies that the phase-shift matrix can be adjusted per slot, denoted by $\mathbf{\Phi}_k = \text{diag}\{e^{j\theta_1[k]}, \ldots, e^{j\theta_{N_s}[k]}\}$, $k = 1, \ldots, K$ with the time-selective phase shift $\theta_n[k]$. The received signal vector for user k is given by

$$\mathbf{y}_k = \left(\mathbf{f}\mathbf{\Phi}_k\mathbf{g}_k + d_k\right)s_k + \mathbf{n}, \tag{12}$$

where d_k is the k^{th} element of $\mathbf{d}$. The phase of each reflected signal should be tuned to align with the phase of the LOS signal for coherent combining at the receiver. Thus, it is not hard to derive that the optimal phase-shift matrix equals

$$\mathbf{\Phi}_k^{\star} = \text{diag}\left\{e^{j\left(\arg(d_k)-\arg\left(\text{diag}(\mathbf{f})\mathbf{g}_k\right)\right)}\right\}, \tag{13}$$

where $\arg(\cdot)$ stands for the phase of a complex scalar or vector. It results in a per-user rate of

$$R_k = \frac{1}{K}\log\left(1+\left|\sum_{n=1}^{N_s}|f_n||g_{n,k}|+|d_k|\right|^2\frac{P_u}{\sigma_n^2}\right), \tag{14}$$

where f_n denotes the channel coefficient between the BS and reflecting element n, and $g_{n,k}$ denotes the channel coefficient between reflecting element n and user k. Thereby, the sum rate of the TDMA-RIS system can be computed by

$$C_{tdma} = \sum_{k=1}^{K}\frac{1}{K}\log\left(1+\frac{P_u\left|\sum_{n=1}^{N_s}|f_n||g_{n,k}|+|d_k|\right|^2}{\sigma_n^2}\right), \tag{15}$$

where the factor $1/K$ is due to the orthogonal partitioning of the time resource.

2) FDMA-RIS: The system bandwidth is split into K orthogonal subchannels, and each user occupies a subchannel over the entire time. Unlike the *time-selective* phase shifting in TDMA, the RIS is not *frequency-selective* due to the hardware limitation. It implies that the surface can be optimized at most for a particular user, whereas other users suffer from phase-unaligned reflection. If the RIS aids the signal transmission of a dedicated user $\hat{k}$, the optimal phase-shift matrix $\mathbf{\Phi}_{\hat{k}}^{\star}$ can be obtained from (13). Its achievable sum rate is calculated by

$$\begin{aligned} C_{fdma} &= \sum_{k=1}^{K}\frac{1}{K}\log\left(1+\frac{P_u\left|\mathbf{f}\mathbf{\Phi}_{\hat{k}}^{\star}\mathbf{g}_k+d_k\right|^2}{\sigma_n^2}\right) \\ &= \frac{1}{K}\log\left(1+\frac{P_u\left|\sum_{n=1}^{N_s}|f_n||g_{n,\hat{k}}|+|d_{\hat{k}}|\right|^2}{\sigma_n^2}\right) \\ &\quad+\sum_{k\neq\hat{k}}\frac{1}{K}\log\left(1+\frac{P_u\left|\mathbf{f}\mathbf{\Phi}_{\hat{k}}^{\star}\mathbf{g}_k+d_k\right|^2}{\sigma_n^2}\right). \end{aligned} \tag{16}$$

Tuning the RIS to optimize different users yields different performance. The best user that maximizes the sum rate can be determined by exhaustively selecting each user as the target:

$$\hat{k} = \arg\max_{k\in\{1,2,\ldots,K\}} C_{fdma}. \tag{17}$$

In addition to the exhaustive search, the simplest way is to randomly select a user.

B. Joint Transmission

From the information-theoretic perspective, OMA is inefficient because each user utilizes only a fraction of the available time-frequency resource. With this regard, we propose a joint-transmission scheme for a RIS-aided MU-MIMO system, where all users transmit their signals simultaneously over the same time-frequency resource.

Unlike OMA, where the RIS is tuned for a particular user, the phase-shift matrix in JT needs to be optimized based on the CSI of all users. Define $\mathbf{q} = [q_1, q_2, \ldots, q_{N_s}]^H$ with $q_n = e^{j\theta_n}$, $n = 1, \ldots, N_s$ and $\boldsymbol{\chi} = \text{diag}(\mathbf{f})\mathbf{G} \in \mathbb{C}^{N_s \times K}$, we have $\mathbf{f}\boldsymbol{\Phi}\mathbf{G} = \mathbf{q}^H\boldsymbol{\chi} \in \mathbb{C}^{1\times K}$. Thus, the objective function in (11) is transferred to $\|\mathbf{f}\boldsymbol{\Phi}\mathbf{G} + \mathbf{d}\|^2 = \left\|\mathbf{q}^H\boldsymbol{\chi} + \mathbf{d}\right\|^2$, resulting in

$$\begin{aligned} \max_{\mathbf{q}} \quad & \mathbf{q}^H\boldsymbol{\chi}\boldsymbol{\chi}^H\mathbf{q} + \mathbf{q}^H\boldsymbol{\chi}\mathbf{d}^H + \mathbf{d}\boldsymbol{\chi}^H\mathbf{q} + \|\mathbf{d}\|^2 \\ \text{s.t.} \quad & |q_n|^2 = 1, \ \forall n = 1, \ldots, N_s, \end{aligned} \tag{18}$$

which is a non-convex QCQP problem [92]. Introducing an auxiliary variable t, (18) can be homogenized as

$$\begin{aligned} & \max_{\mathbf{q}} \quad \left\|t\mathbf{q}^H\boldsymbol{\chi} + \mathbf{d}\right\|^2 \\ = & \max_{\mathbf{q}} \quad t^2\mathbf{q}^H\boldsymbol{\chi}\boldsymbol{\chi}^H\mathbf{q} + t\mathbf{q}^H\boldsymbol{\chi}\mathbf{d}^H + t\mathbf{d}\boldsymbol{\chi}^H\mathbf{q} + \|\mathbf{d}\|^2, \end{aligned} \tag{19}$$

Defining

$$\mathbf{C} = \begin{bmatrix} \boldsymbol{\chi}\boldsymbol{\chi}^H & \boldsymbol{\chi}\mathbf{d}^H \\ \mathbf{d}\boldsymbol{\chi}^H & \|\mathbf{d}\|^2 \end{bmatrix}, \ \mathbf{v} = \begin{bmatrix} \mathbf{q} \\ t \end{bmatrix}, \tag{20}$$

(19) equals to

$$\begin{aligned} \max_{\mathbf{v}} \quad & \mathbf{v}^H\mathbf{C}\mathbf{v} \\ \text{s.t.} \quad & |q_n|^2 = 1, \ \forall n = 1, \ldots, N_s \\ & |t|^2 = 1. \end{aligned} \tag{21}$$

Let $\mathbf{V} = \mathbf{v}\mathbf{v}^H$, we have $\mathbf{v}^H\mathbf{C}\mathbf{v} = \text{Tr}(\mathbf{C}\mathbf{V})$, where $\text{Tr}(\cdot)$ denotes the trace of a matrix. As a result, (21) is reformulated as

$$\begin{aligned} \max_{\mathbf{V}} \quad & \text{Tr}\,(\mathbf{C}\mathbf{V}) \\ \text{s.t.} \quad & \mathbf{V}_{n,n} = 1, \ \forall n = 1, \ldots, N_s, \\ & \mathbf{V} \succ 1 \end{aligned} \tag{22}$$

where $\mathbf{V}_{n,n}$ means the n^{th} diagonal element of $\mathbf{V}$, and $\succ$ stands for a positive semi-definite matrix. The optimization formula is transformed to a semi-definite program, whose globally optimal solution $\mathbf{V}^\star$ can be efficiently solved by available numerical algorithms such as CVX in MATLAB [94].

Conduct the eigenvalue decomposition $\mathbf{V}^\star = \mathbf{U}\boldsymbol{\Sigma}\mathbf{U}^H$, where $\mathbf{U}$ is a unitary matrix and $\boldsymbol{\Sigma}$ is a diagonal matrix, both with the size $(N_s + 1) \times (N_s + 1)$. A sub-optimal solution for the optimization problem is given by

$$\bar{\mathbf{v}} = \mathbf{U}\boldsymbol{\Sigma}^{1/2}\mathbf{r}, \tag{23}$$

where $\mathbf{r}$ is a Gaussian random vector generated according to $\mathbf{r} \in \mathcal{CN}(\mathbf{0}, \mathbf{I}_{N_s+1})$. Finally, the solution to the optimization problem can be determined as

$$\boldsymbol{\Phi}_{JT}^\star = \text{diag}\left\{e^{j\arg\left(\left[\frac{\bar{\mathbf{v}}}{\bar{v}_{N_s+1}}\right]_{1:N_s}\right)}\right\}, \tag{24}$$

where $[\cdot]_{1:N_s}$ denotes a sub-vector extracting the first N_s elements, and $\bar{v}_{N_s+1}$ is the last element of $\bar{\mathbf{v}}$.

Thus, the sum capacity of JT is computed as

$$C_{JT} = \log\left(1 + \frac{\left\|\mathbf{f}\boldsymbol{\Phi}_{JT}^\star\mathbf{G} + \mathbf{d}\right\|^2 P_u}{\sigma_n^2}\right), \tag{25}$$

where the factor $1/K$ in (15) and (16) is avoided due to the full exploitation of the time-frequency resource in JT. Ideally, the applied phase-shift matrix can optimally optimize the reflection for all users simultaneously, providing an upper performance bound of JT as

$$C_{Upper} = \log\left(1 + \frac{\sum_{k=1}^{K}\left|\sum_{n=1}^{N_s}|f_n||g_{n,k}| + |d_k|\right|^2 P_u}{\sigma_n^2}\right). \tag{26}$$

The joint transmission for RIS-aided MU-MIMO systems is depicted also in Algorithm 1.

Algorithm 1: Joint RIS Transmission

Initialization: $\mathbf{q} \leftarrow [q_1, q_2, \ldots, q_{N_s}]^H$ with $q_n = e^{j\theta_n}$;

$\mathbf{v} \leftarrow \left[\mathbf{q}^T, t\right]^T$ with $|t| = 1$;

$\mathbf{V} \leftarrow \mathbf{v}\mathbf{v}^H$;

foreach *Transmission Block* **do**

Estimate $\mathbf{f}$, $\mathbf{d}$, and $\mathbf{G}$;

$\boldsymbol{\chi} \leftarrow \mathrm{diag}(\mathbf{f})\mathbf{G}$;

$\mathbf{C} \leftarrow \begin{bmatrix} \boldsymbol{\chi}\boldsymbol{\chi}^H & \boldsymbol{\chi}\mathbf{d}^H \\ \mathbf{d}\boldsymbol{\chi}^H & \|\mathbf{d}\|^2 \end{bmatrix}$;

Solve (22) using CVX;

Decompose $\mathbf{V}^\star = \mathbf{U}\boldsymbol{\Sigma}\mathbf{U}^H$;

$\bar{\mathbf{v}} \leftarrow \mathbf{U}\boldsymbol{\Sigma}^{1/2}\mathbf{r}$, where $\mathbf{r} \in \mathcal{CN}(\mathbf{0}, \mathbf{I}_{N_s+1})$;

Adjust RIS with $\boldsymbol{\Phi}_{JT}^\star = \mathrm{diag}\left\{e^{j\arg\left(\left[\frac{\bar{\mathbf{v}}}{\bar{v}_{N_s+1}}\right]_{1:N_s}\right)}\right\}$;

All users jointly transmit;

end

Algorithm 2: Opportunistic RIS Transmission

foreach *Transmission Block* **do**

Estimate $\mathbf{f}$, $\mathbf{d}$, and $\mathbf{G}$;

foreach *User* k **do**

$\boldsymbol{\Phi}_k^\star \leftarrow e^{j\left(\arg(d_k) - \arg\left(\mathrm{diag}(\mathbf{f})\mathbf{g}_k\right)\right)}$;

$R_k^\star \leftarrow \log\left[1 + \frac{\|\mathbf{f}\boldsymbol{\Phi}\mathbf{g}_k + d_k\|^2 P_u}{\sigma_n^2}\right]$;

end

$k^\star \leftarrow \arg\max_{k=1,\ldots,K}(R_k^\star)$;

$k^\star$ transmits while $k \neq k^\star$ turn off;

end

C. Opportunistic Transmission

If multiple users fade independently, the probability that one of the users experiences strong channel quality is substantially higher than that of a single user. Therefore, the sum capacity can be improved by exploiting the effect of multi-user diversity. By assigning the shared transmission resource only to the best user, the total throughput of the system is maximized. The more users the system can schedule, the stronger channel the best user probably has. Based on this observation, we propose an opportunistic scheme for the RIS-aided MU-MIMO system.

Accordingly, the *single-user bound* is rewritten as

$$R_k < \log\left[1 + \frac{\|\mathbf{f}\mathbf{\Phi}\mathbf{g}_k + d_k\|^2 P_u}{\sigma_n^2}\right], \ \forall\, k. \tag{27}$$

The optimal phase-shift matrix is given by

$$\mathbf{\Phi}_k^{\star} = \mathrm{diag}\left\{e^{j\left(\arg(d_k) - \arg\left(\mathrm{diag}(\mathbf{f})\mathbf{g}_k\right)\right)}\right\}. \tag{28}$$

Substituting (28) into (27) yields the maximal achievable rate of user k, denoted by $R_k^{\star}$. The philosophy of the opportunistic transmission is to determine the best user with the largest rate, mathematically,

$$k^{\star} = \arg \max_{k\in\{1,\ldots,K\}} \left(R_k^{\star}\right), \tag{29}$$

and then assigning the shared transmission resource merely to $k^{\star}$. Other users turn off while the best user transmits its signal. The sum capacity of OT is computed by

$$\begin{aligned} C_{OT} &= \max_{k\in\{1,\ldots,K\}} \left(\log\left[1 + \frac{\left\|\mathbf{f}\mathbf{\Phi}_k^{\star}\mathbf{g}_k + d_k\right\|^2 P_u}{\sigma_n^2}\right]\right) \\ &= \max_{k\in\{1,\ldots,K\}} \left(\log\left(1 + \frac{\left|\sum_{n=1}^{N_s} |f_n||g_{n,k}| + |d_k|\right|^2 P_u}{\sigma_n^2}\right)\right). \end{aligned} \tag{30}$$

V. Numerical results

Monte-Carlo simulations are conducted to evaluate the performance of joint and opportunistic transmission in an RIS-aided MU-MIMO system. This section first elaborates the simulation parameters and then provides some representative numerical results in terms of the sum throughput. Without loss of generality, we established a simulation scenario as shown in Fig.2. The BS is located at the original point of the coordinate system, while the RIS with $N_s = 200$ reconfigurable elements is deployed in the middle of the cell edge. Cell-center users distribute randomly over a square area with the side length of $X_2 = 300\,\mathrm{m}$, while cell-edge users distribute randomly over another square area from $X_1 = 250\,\mathrm{m}$ to $X_3 = 500\,\mathrm{m}$. The power constraint of the UE is assumed to be $P_u = 1.0\mathrm{W}$ over a signal bandwidth of 1MHz. The noise power density is $-174\mathrm{dBm/Hz}$ with the noise figure 9dB. The large-scale fading is distance-dependent, computed by $\sigma_c^2 = 10^{\frac{\mathcal{L}+\mathcal{S}}{10}}$, where $\mathcal{L}$ denotes the path loss, and $\mathcal{S} \sim \mathcal{N}(0, \sigma_{sd}^2)$ is the Log-Normal shadowing with a standard derivation $\sigma_{sd} = 8\mathrm{dB}$. The COST-Hata model (refer to [48]) is employed to determine $\mathcal{L}$ using the break points of 10m and 50m, the carrier frequency of $f_c = 1.9\mathrm{GHz}$, the BS/RIS height of 15m, and the UE height of 1.65m. Due to the line of sight, the path loss of the BS-RIS channel can be calculated by $\mathcal{L}_0/d^{-\alpha}$, where $\mathcal{L}_0 = -30\,\mathrm{dB}$ is the path loss at the reference distance of 1 m, the path-loss exponent $\alpha = 2$, and the Rician factor $\Gamma = 5$.

Our simulation provides a comprehensive comparison among different schemes, including: 1) the conventional direct communications (DC) where the UEs directly access to the BS without the aid of RIS; 2) FDMA that randomly selects a user

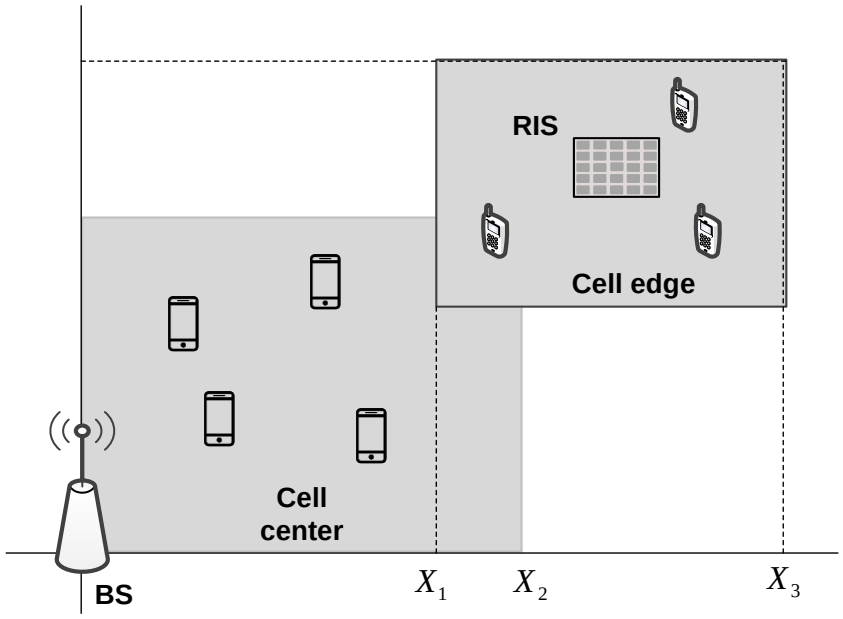

Fig. 2. Simulation setup of a multi-user RIS system, where the cell coverage is comprised of a cell-center area and a cell-edge area.

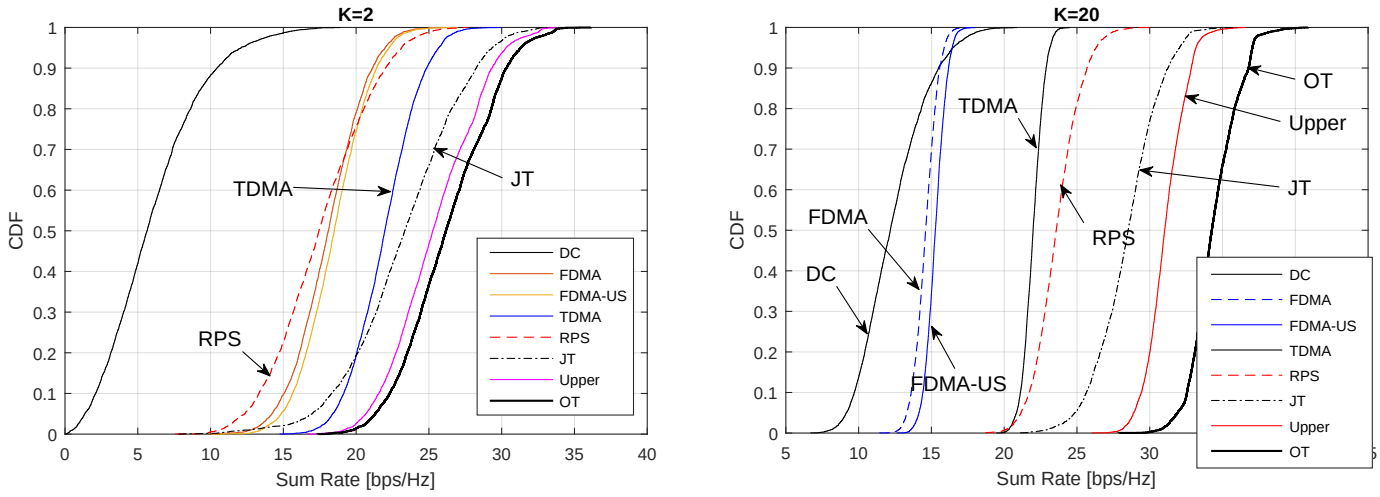

(a) (b)

Fig. 3. Performance comparison of different transmission schemes in the uplink of a RIS-aided multi-user system: (a) CDFs in terms of the sum rate with two users, and (b) CDFs in terms of the sum rate with twelve users.

for optimizing the RIS coefficients; 3) FDMA-US means exhaustive search to determine the best user for optimizing the RIS coefficients; 4) TDMA; 5) random phase shift (RPS) where the phase shifts of the RIS elements are *randomly* set; 6) JT; 7) The upper bound of the JT, see (26); and 8) OT.

Cumulative distribution function (CDF) of the sum rate is employed as the performance metric. To provide some insights, we first compare the CDFs of different schemes with the minimal number of $K = 2$ users, consisting of a cell-center user and a cell-edge user. As shown in Fig.3a, the conventional DC system achieves the 50%-likely or median sum rate of 5.6 bps/Hz.

The deployment of RIS can substantially boost the system performance, where FDMA without and with user selection have a sum rate of around 18.1 bps/Hz and 18.5 bps/Hz, respectively. TDMA obviously outperforms FDMA with a 50%-likely sum rate of approximately 22 bps/Hz. That is because the RIS can provide time-selective reflection dedicated for each TDMA user, whereas only the signal transmission of a single FDMA user can get aids owing to the lack of frequency-selective reflection. As we expected, JT is superior to TDMA, where the 50%-likely rate is increased to approximately 23.3 bps/Hz. That is because the signal transmission of each JT user fully exploits the time-frequency resource, in contrast to $1/K$ degree of freedom per OMA user. If the phase shifts are random, the result is 17.4 bps/Hz, which justifies the effectiveness of the joint reflection optimization. The multi-user gain due to opportunistic user selection is solid, where OT has a median rate of 26.2 bps/Hz, better than the upper performance bound of JT. In addition, we also illustrate the performance comparison in the case of $K = 20$ users, as illustrated in Fig.3b, where similar conclusions can be drawn from the numerical results. It is noted that the multi-user gain of OT becomes large with the increasing number of users.

VI. Conclusions

Based on the insights provided by the capacity analysis, we proposed two novel schemes, i.e., *joint transmission* and *opportunistic transmission* for RIS-aided multi-user MIMO communications system. The superiority of the proposed schemes over the conventional orthogonal multiple access in terms of achievable sum rate was extensively justified through Monte-Carlo simulation. Particularly, opportunistic transmission has low complexity since it relies only on the best user selection, but obviously outperforming joint transmission, especially when the number of users becomes large. Regardless of high complexity raised by the semidefinite relaxation of quadratically constrained quadratic program, joint transmission still cannot compete with opportunistic transmission. The findings of this paper inspires us to further exploit multi-user diversity and opportunistic communications in RIS-aided systems. on

References

[1] T. Kaiser *et al.*, "Cognitive radio – a current snapshot and some thoughts on commercialization for future cellular systems," *J. Signal Process. Syst.*, vol. 73, no. 3, pp. 217–225, Dec. 2013.

[2] W. Jiang *et al.*, "Key issues towards beyond LTE-Advanced systems with cognitive radio," in *Proc. IEEE 2013 Workshop on Sign. Proc. Adv. in Wireless Commun. (SPAWC)*, Darmstadt, Germany, Jun. 2013, pp. 510–514.

[3] H. Cao *et al.*, "The design of an LTE-A system enhanced with cognitive radio," in *Proc. Eur. Signal Process. Conf. (EUSIPCO)*, Marrakech, Morocco, Sep. 2013, pp. 1–6.

[4] M. D. Mueck *et al.*, "Novel spectrum usage paradigms for 5G," White Paper, IEEE Technical Committee on Cognitive Networks (TCCN) Special Interest Group on *Cognitive Radio for 5G*, Nov. 2014.

[5] J. P. Santos *et al.*, "SELFNET framework self-healing capabilities for 5G mobile networks," *Trans. Emerg. Telecommu. Techno.*, vol. 27, no. 9, pp. 1225–1232, Sep. 2016.

[6] P. Neves *et al.*, "The SELFNET approach for autonomic management in an NFV/SDN networking paradigm," *Int. J. Distrib. Sensor Netw.*, pp. 1–17, Feb. 2016.

[7] W. Jiang *et al.*, "Experimental results for Artificial Intelligence-based self-organized 5G networks," in *Proc. IEEE Int. Symp. on Pers., Indoor and Mobile Radio Commun. (PIMRC)*, Montreal, Canada, Oct. 2017.

[8] ——, "Intelligent network management for 5G systems: The SELFNET approach," in *Proc. IEEE Eur. Conf. on Netw. and Commun. (EUCNC)*, Oulu, Finland, Jun. 2017, pp. 109–113.

[9] ——, "Autonomic network management for software-define and virtualized 5G systems," in *Proc. Eur. Wireless*, Dresden, Germany, May 2017.

[10] W. Jiang, "Device-to-device based cooperative relaying for 5G network: A comparative review," *ZTE Communications*, vol. 15, pp. 60–66, Jun. 2017.

[11] W. Jiang *et al.*, "A SON decision-making framework for intelligent management in 5G mobile networks," in *Proc. IEEE Int. Conf. on Compu. and Commun. (ICCC)*, Chengdu, China, Dec. 2017.

[12] ——, "An SDN/NFV proof-of-concept test-bed for machine learning-based network management," in *Proc. IEEE Int. Conf. on Compu. and Commun. (ICCC)*, Chengdu, China, Dec. 2018.

[13] W. Jiang, M. Strufe, and H. Schotten, "Machine learning-based framework for autonomous network management in 5G systems," in *Proc. 2018 Eur. Conf. on Netw. and Commun. (EuCNC)*, Ljubljana, Slovenia, Jun. 2018.

[14] W. Jiang, S. D. Anton, and H. D. Schotten, "Intelligence slicing: A unifed framework to integrate artificial intelligence into 5G networks," in *Proc. 2019 12th IFIP Wireless and Mobile Netw. Conf. (WMNC)*, Paris, France, Sep. 2019, pp. 227–232.

[15] W. Jiang and F.-L. Luo, "Editorial: Special topic on computational radio intelligence: One key for 6G wireless," *ZTE Communications*, vol. 17, no. 4, pp. 1–3, Dec. 2019.

[16] W. Jiang *et al.*, "The road towards 6G: A comprehensive survey," *IEEE Open J. Commun. Society*, vol. 2, pp. 334–366, Feb. 2021.

[17] W. Jiang and H. D. Schotten, "The kick-off of 6G research worldwide: An overview," in *Proc. 2021 Seventh IEEE Int. Conf. on Comput. and Commun. (ICCC)*, Chengdu, China, Dec. 2021.

[18] W. Jiang and F.-L. Luo, *6G Key Technologies: A Comprehensive Guide*. New York, USA: IEEE Press and John Wiley&Sons, 2022.

[19] W. Jiang and H. Schotten, "Neural network-based fading channel prediction: A comprehensive overview," *IEEE Access*, vol. 7, pp. 118 112–118 124, Aug. 2019.

[20] W. Jiang and H. D. Schotten, "Deep learning for fading channel prediction," *IEEE Open J. the Commun. Society*, vol. 1, pp. 320–332, Mar. 2020.

[21] ——, "Multi-antenna fading channel prediction empowered by artificial intelligence," in *Proc. 2018 IEEE Veh. Technol. Conf. (VTC-Fall)*, Chicago, USA, Aug. 2018.

[22] W. Jiang and H. Schotten, "Neural network-based channel prediction and its performance in multi-antenna systems," in *Proc. 2018 IEEE Veh. Technol. Conf. (VTC-Fall)*, Chicago, USA, Aug. 2018.

[23] W. Jiang and H. D. Schotten, "A comparison of wireless channel predictors: Artificial Intelligence versus Kalman filter," in *Proc. 2019 IEEE Int. Commun. Conf. (ICC)*, Shanghai, China, May 2019.

[24] W. Jiang and H. Schotten, "Recurrent neural network-based frequency-domain channel prediction for wideband communications," in *Proc. 2019 IEEE Veh. Technol. Conf. (VTC-Spring)*, Kuala Lumpur, Malaysia, Apr. 2019.

[25] W. Jiang, M. Strufe, and H. Schotten, "Long-range fading channel prediction using recurrent neural network," in *Proc. 2020 IEEE Consum. Commun. and Netw. Conf.*, Las Vegas, USA, Jan. 2020.

[26] W. Jiang and H. D. Schotten, "A deep learning method to predict fading channel in multi-antenna systems," in *Proc. 2020 IEEE Veh. Technol. Conf. (VTC-Spring)*, Antwerp, Belgium, May 2020.

[27] ——, "Recurrent neural networks with long short-term memory for fading channel prediction," in *Proc. 2020 IEEE Veh. Technol. Conf. (VTC-Spring)*, Antwerp, Belgium, May 2020.

[28] W. Jiang, H. Schotten, and J.-Y. Xiang, "Neural network based wireless channel prediction," in *Machine Learning for Future Wireless Communications*, F. L. Luo, Ed. United Kindom: John Wiley&Sons and IEEE Press, 2020, ch. 16.

[29] A. M. Seid *et al.*, "Multi-agent DRL for task offloading and resource allocation in multi-UAV enabled IoT edge network," *IEEE Trans. Netw. Serv. Manag.*, vol. 18, no. 4, pp. 4531 – 4547, Dec. 2021.

[30] G. Sun *et al.*, "Dynamic resource reservation for ultra-low latency IoT air-interface slice," *KSII Trans. Internet Info. Syst.*, vol. 11, no. 7, pp. 3309–3328, Jun. 2017.

[31] ——, "Dynamic reservation and deep reinforcement learning based autonomous resource slicing for virtualized radio access networks," *IEEE Access*, vol. 7, pp. 45 758–45 772, Apr. 2019.

[32] ——, "Resource slicing and customization in ran with dueling deep q-network," *J. Netw. Computer App.*, vol. 157, May 2020.

[33] ——, "Autonomous resource slicing for virtualized vehicular networks with d2d communications based on deep reinforcement learning," *IEEE Syst. J.*, vol. 14, no. 4, pp. 4694–4705, Dec. 2020.

[34] ——, "Autonomous resource provisioning and resource customization for mixed traffics in virtualized radio access network," *IEEE Syst. J.*, vol. 13, no. 3, pp. 2454 – 2465, Sep. 2019.

[35] ——, "Transfer learning for autonomous cell activation based on relational reinforcement learning with adaptive reward," *IEEE Syst. J.*, vol. 16, no. 1, pp. 1044 – 1055, Mar. 2021.

[36] Y. H. Yacob *et al.*, "An optimal incentive mechanism for blockchain-enabled content caching in device-to-device communication," in *Proc. 2022 IEEE Int. Conf. Computing, Commun., Perception Quantum Techno. (CCPQT 2022)*, Xiamen, China, Aug. 2022.

[37] H. Cao *et al.*, "A robust radio access technology classification scheme with practical considerations," in *Proc. IEEE Int. Symp. on Pers., Indoor and Mobile Radio Commun. (PIMRC)*, London, UK, Sep. 2013, pp. 36–40.

[38] H. cao *et al.*, "Multi-channel robust spectrum sensing with low-complexity filter bank realization," in *Proc. IEEE Int. Symp. on Pers., Indoor and Mobile Radio Commun. (PIMRC)*, London, UK, Sep. 2013, pp. 861–865.

[39] H. Cao, W. Jiang, and T. Kaiser, "Parallel in-band signal detection with self-interference suppression for cognitive LTE," in *Proc. 2014 IEEE Wireless Commun. and Netw. Conf. (WCNC)*, Istanbul, Turkey, Apr. 2014.

[40] W. Jiang, D. Yu, and Y. Ma, "A tracking algorithm in RFID reader network," in *Proc. 2006 Japan-China Joint Workshop on Frontier of Compu. Sci. and Techno. (FCST)*, Fukushima, Japan, Nov. 2006, pp. 164–171.

[41] W. Jiang and Y. Ma, "Interference analysis of microwave RFID and 802.11b WLAN," in *Proc. 2007 Int. Conf. on Wireless Commun., Netw. and Mobile Computing (WiCOM)*, Shanghai, China, Sep. 2007, pp. 2062–2065.

[42] W. Jiang, "Bit error rate analysis of Wi-Fi and bluetooth under the interference of 2.45GHz RFID," *J. China Universities of Posts and Telecommun.*, vol. 14, pp. 89–93, Oct. 2007.

[43] W. Jiang and H. D. Schotten, "Initial beamforming for millimeter-wave and terahertz communications in 6G mobile systems," in *Proc. 2022 IEEE Wireless Commun. and Netw. Conf. (WCNC)*, Austin, USA, Apr. 2022.

[44] ——, "Initial access for millimeter-wave and terahertz communications with hybrid beamforming," in *Proc. 2022 IEEE Int. Commun. Conf. (ICC)*, Seoul, South Korea, May 2022.

[45] W. Jiang and H. Schotten, "Dual-beam intelligent reflecting surface for millimeter and THz communications," in *Proc. 2022 IEEE 95th Veh. Techno. Conf. (VTC2022-Spring)*, Helsinki, Finland, Jun. 2022.

[46] G. Yuan *et al.*, "Bidirectional branch and bound based antenna selection in massive MIMO systems," in *Proc. 2015 IEEE 23rd Int. Symp. on Pers., Indoor and Mobile Radio Commun. (PIMRC)*, Hongkong, China, Sep. 2015, pp. 563 – 568.

[47] W. Jiang and Y. Wang, "User pairing method, device and system for realizing user scheduling," U.S. Patent 10 212 723, Feb. 19, 2019.

[48] W. Jiang and H. D. Schotten, "Cell-free massive MIMO-OFDM transmission over frequency-selective fading channels," *IEEE Commun. Lett.*, vol. 25, no. 8, pp. 2718 – 2722, Aug. 2021.

[49] W. Jiang and H. Schotten, "Impact of channel aging on zero-forcing precoding in cell-free massive MIMO systems," *IEEE Commun. Lett.*, vol. 25, no. 9, pp. 3114 – 3118, Sep. 2021.

[50] ——, "Opportunistic AP selection in cell-free massive MIMO-OFDM systems," in *Proc. 2022 IEEE 95th Veh. Techno. Conf. (VTC2022-Spring)*, Helsinki, Finland, Jun. 2022.

[51] ——, "Deep learning-aided delay-tolerant zero-forcing precoding in cell-free massive MIMO," in *Proc. 2022 IEEE 96th Veh. Techno. Conf. (VTC2022-Fall)*, London, UK, Sep. 2022.

[52] M. D. Renzo *et al.*, "Smart radio environments empowered by reconfigurable intelligent surfaces: How it works, state of research, and the road ahead," *IEEE J. Sel. Areas Commun.*, vol. 38, no. 11, pp. 2450 – 2525, Nov. 2020.

[53] W. Jiang and H. Schotten, "Multi-user reconfigurable intelligent surface-aided communications under discrete phase shifts," in *Proc. 36th IEEE Int. Workshop on Commun. Qual. and Reliability (CQR 2022)*, Arlington, United States, Sep. 2022.

[54] ——, "Intelligent reflecting vehicle surface: A novel IRS paradigm for moving vehicular networks," in *Proc. 2022 IEEE 40th Military Commun. Conf. (MILCOM 2022)*, Rockville, MA, USA, Nov. 2022.

[55] ——, "Performance impact of channel aging and phase noise on intelligent reflecting surface," *IEEE Commun. Lett.*, vol. 27, no. 1, pp. 347–351, Jan. 2023.

[56] Q. Wu and R. Zhang, "Towards smart and reconfigurable environment: Intelligent reflecting surface aided wireless network," *IEEE Commun. Mag.*, vol. 58, no. 1, pp. 106 – 112, Jan. 2020.

[57] W. Yan *et al.*, "Passive beamforming and information transfer design for reconfigurable intelligent surfaces aided multiuser MIMO systems," *IEEE J. Sel. Areas Commun.*, vol. 38, no. 8, pp. 1793 – 1808, Aug. 2020.

[58] L. You *et al.*, "Energy efficiency and spectral efficiency tradeoff in RIS-aided multiuser MIMO uplink transmission," *IEEE Trans. Signal Process.*, vol. 69, no. 12, pp. 1407 – 1421, Dec. 2020.

[59] Y. Lv, Z. He, and Y. Rong, "Multiuser uplink MIMO communications assisted by multiple reconfigurable intelligent surfaces," *IEEE Commun. Lett.*, vol. 25, no. 12, pp. 3975 – 3979, Dec. 2021.

[60] B. Zheng, C. You, and R. Zhang, "Double-IRS assisted multi-user MIMO: Cooperative passive beamforming design," *IEEE Trans. Wireless Commun.*, vol. 20, no. 7, pp. 4513 – 4526, Jul. 2021.

[61] L. You *et al.*, "Reconfigurable intelligent surfaces-assisted multiuser MIMO uplink transmission with partial CSI," *IEEE Trans. Wireless Commun.*, vol. 20, no. 9, pp. 5613 – 5627, Sep. 2021.

[62] H. Niu *et al.*, "Double intelligent reflecting surface-assisted multi-user MIMO mmwave systems with hybrid precoding," *IEEE Trans. Veh. Technol.*, vol. 71, no. 2, pp. 1575 – 1587, Feb. 2022.

[63] H. U. Rehman *et al.*, "Modulating intelligent surfaces for multiuser MIMO systems: Beamforming and modulation design," *IEEE Trans. Commun.*, vol. 70, no. 5, pp. 3234 – 3249, May 2022.

[64] J. Hu *et al.*, "Reconfigurable intelligent surface based uplink MU-MIMO symbiotic radio system," *IEEE Trans. Wireless Commun.*, Aug. 2022, early Access.

[65] H. Liu, X. Yuan, and Y.-J. A. Zhang, "Matrix-calibration-based cascaded channel estimation for reconfigurable intelligent surface assisted multiuser MIMO," *IEEE J. Sel. Areas Commun.*, vol. 38, no. 11, pp. 2621 – 2636, Nov. 2020.

[66] B. Zheng, C. You, and R. Zhang, "Efficient channel estimation for double-irs aided multi-user MIMO system," *IEEE Trans. Commun.*, vol. 69, no. 6, pp. 3818 – 3832, Jun. 2021.

[67] Q. Wu and R. Zhang, "Intelligent reflecting surface enhanced wireless network via joint active and passive beamforming," *IEEE Trans. Wireless Commun.*, vol. 18, no. 11, pp. 5394 – 5409, Nov. 2019.

[68] X. Yang, W. Jiang, and B. Vucetic, "A random beamforming technique for omnidirectional coverage in multiple-antenna systems," *IEEE Trans. Veh. Technol.*, vol. 62, no. 3, pp. 1420 – 1425, Mar. 2013.

[69] W. Jiang and X. Yang, "Method and apparatus for transmitting broadcast signal," U.S. Patent Application 13/685 426, Nov. 26, 2012.

[70] X. Yang, W. Jiang, and B. Vucetic, "A random beamforming technique for broadcast channels in multiple antenna systems," in *Proc. 2011 IEEE Veh. Techno. Conf. (VTC Fall)*, San Francisco, USA, Sep. 2011.

[71] X. Yang and W. Jiang, "Method and apparatus for cell/sector coverage of a public channel through multiple antennas," U.S. Patent 8 537 785, Sep. 17, 2013.

[72] ——, "Method, apparatus, and system for controlling multi-antenna signal transmission," U.S. Patent Application 13/654 743, Oct. 18, 2012.

[73] W. Jiang and X. Yang, "An enhanced random beamforming scheme for signal broadcasting in multi-antenna systems," in *Proc. 2012 IEEE 23rd Int. Symp. on Pers., Indoor and Mobile Radio Commun. (PIMRC)*, Sydney, NSW, Australia, Sep. 2012, pp. 2055 – 2060.

[74] X. Yang and W. Jiang, "Method and apparatus for transmitting signals in a multiple antennas system," U.S. Patent 8 170 132, May 1, 2012.

[75] W. Jiang, H. Cao, and T. Kaiser, "Opportunistic space-time coding to exploit cooperative diversity in fast-fading channels," in *Proc. 2014 IEEE Int. Commun. Conf. (ICC)*, Sydney, NSW, Australia, Jun. 2014, pp. 4814–4819.

[76] W. Jiang *et al.*, "Opportunistic relaying over aerial-to-terrestrial and device-to-device radio channels," in *Proc. 2014 IEEE Intl. Conf. on Commun. (ICC)*, Sydney, Australia, Jul. 2014, pp. 206–211.

[77] ——, "Achieving high reliability in aerial-terrestrial networks: Opportunistic space-time coding," in *Proc. IEEE Eur. Conf. on Net. and Commun. (EUCNC)*, Bologne, Italy, Jun. 2014.

[78] W. Jiang, H. Cao, and T. Kaiser, "An MGF-based performance analysis of opportunistic relay selection with outdated CSI," in *Proc. 2014 IEEE 79th Veh. Technol. Conf. (VTC-Spring)*, Seoul, South Korea, May 2014.

[79] ——, "Analysis of generalized selection combining in cooperative networks with outdated CSI," in *Proc. 2014 IEEE Wireless Commun. and Netw. Conf. (WCNC)*, Istanbul, Turkey, Apr. 2014.

[80] ——, "Power optimal allocation in decode-and-forward opportunistic relaying," in *Proc. 2014 IEEE Wireless Commun. and Netw. Conf. (WCNC)*, Istanbul, Turkey, Apr. 2014.

[81] W. Jiang, T. Kaiser, and A. J. H. Vinck, "A robust opportunistic relaying strategy for co-operative wireless communications," *IEEE Trans. Wireless Commun.*, vol. 15, no. 4, pp. 2642–2655, Apr. 2016.

[82] W. Jiang and H. Schotten, "Predictive relay selection: A cooperative diversity scheme using deep learning," in *Proc. 2021 IEEE Wireless Commun. and Netw. Conf. (WCNC)*, Nanjing, China, Mar. 2021.

[83] W. Jiang and H. D. Schotten, "A simple cooperative diversity method based on deep-learning-aided relay selection," *IEEE Trans. Veh. Technol.*, vol. 70, no. 5, pp. 4485 – 4500, May 2021.

[84] W. Jiang and Z. Zhao, "Low-complexity spectral precoding for rectangularly pulsed OFDM," in *Proc. 2012 IEEE Veh. Technol. Conf. (VTC-Fall)*, Quebec City, QC, Canada, Sep. 2012.

[85] W. Jiang and M. Schellmann, "Suppressing the out-of-band power radiation in multi-carrier systems: A comparative study," in *Proc. 2012 IEEE Global Commun. Conf. (Globecom)*, Anaheim, CA, USA, Dec. 2012, pp. 1477 – 1482.

[86] W. Jiang, "Multicarrier transmission schemes in cognitive radio," in *Proc. 2012 Int. Symp. on Signals, Syst., and Electron. (ISSSE)*, Potsdam, Germany, Oct. 2012.

[87] G. Sun, X. Zhou, and W. Jiang, "Method and apparatus for sending signals," U.S. Patent 9 031 155, May 12, 2015.

[88] W. Jiang and T. Kaiser, "From OFDM to FBMC: Principles and Comparisons," in *Signal Processing for 5G: Algorithms and Implementations*, F. L. Luo and C. Zhang, Eds. United Kindom: John Wiley&Sons and IEEE Press, 2016, ch. 3.

[89] G. Sun, W. Jiang, and G. Zhao, "Method for reducing inter-femtocell interference and femtocell base station," U.S. Patent 9 369 244, Jun. 14, 2016.

[90] W. Jiang, "Method for dynamically setting virtual subcarriers, receiving method, apparatus and system," U.S. Patent 9 319 885, Apr. 19, 2016.

[91] D. Tse and P. Viswanath, *Fundamentals of Wireless Communication*. Cambridge, United Kingdom: Cambridge University Press, Sep. 2005.

[92] N. Sidiropoulos, T. Davidson, and Z.-Q. Luo, "Transmit beamforming for physical-layer multicasting," *IEEE Trans. Signal Process.*, vol. 54, no. 6, pp. 2239 – 2251, Jun. 2006.

[93] L. Zhang *et al.*, "Space-time-coding digital metasurfaces," *Nature Commun.*, vol. 9, no. 1, p. 4334, 1998.

[94] M. Grant and S. Boyd, "CVX: Matlab software for disciplined convex programming, version 2.1," http://cvxr.com/cvx, Mar. 2014.